High operational and environmental stability of high-mobility conjugated polymer field-effect transistors achieved through the use of molecular additives

Mark Nikolka[1*], Iyad Nasrallah[1*], Bradley Rose[3], Mahesh Kumar Ravva[3], Katharina Broch[1], David Harkin[1], Jerome Charmet[5], Michael Hurhangee[2], Adam Brown[1], Steffen Illig[1], Patrick Too[4], Jan Jongman[4], Iain McCulloch[2,3], Jean-Luc Bredas[3] and Henning Sirringhaus[1]

[1]Optoelectronics Group, Cavendish Laboratory, JJ Thomson Avenue, Cambridge CB3 0HE, United Kingdom.

[2]Department of Chemistry and Centre for Plastic Electronics, Imperial College London, London SW7 2AZ, United Kingdom.

[3] Solar & Photovoltaics Engineering Research Center, Division of Physical Science and Engineering, King Abdullah University of Science and Technology (KAUST), Thuwal 23955-6900, Kingdom of Saudi Arabia.

[4]FlexEnable Ltd, 34 Cambridge Science Park, Cambridge, CB4 0FX, United Kingdom.

[5]Department of Chemistry, Lensfield Road, Cambridge, CB2 1EW, United Kingdom.

[*]equal contribution

Due to their low-temperature processing properties and inherent mechanical flexibility, conjugated polymer field-effect transistors (FETs) are promising candidates for enabling flexible electronic circuits and displays. Much progress has been made on materials performance; however, there remain significant concerns about operational and environmental stability, particularly in the context of applications that require a very high level of threshold voltage

stability, such as active-matrix addressing of organic light-emitting diode (OLED) displays. Here, we investigate the physical mechanisms behind operational and environmental degradation of high mobility, p-type polymer FETs and demonstrate an effective route to improve device stability. We show that water incorporated in nanometer sized voids within the polymer microstructure is the key factor in charge trapping and device degradation. By inserting molecular additives that displace water from these voids, it is possible to increase the stability as well as uniformity to a high level sufficient for demanding industrial applications.

The longstanding research efforts to discover high-mobility organic semiconductors have resulted in several families of materials that exceed the mobility performance of common thin-film inorganic semiconductors, such as amorphous silicon[1,2,3]. With polycrystalline molecular semiconductors the key challenge is now to achieve the required device uniformity for large-area applications, such as displays. With conjugated polymers that show high field-effect mobilities > 1cm^2/Vs in nearly amorphous microstructures[4,2,5], device uniformity over large-areas can be excellent but the reduced crystallinity and the associated faster diffusion of extrinsic species such as oxygen or water makes these materials prone to environmental and operational degradation[6]. The presence of water has been shown to cause strong electron trapping in n-type organic FETs[7] and diodes[8]. Water at the interface has also been identified as a cause of threshold voltage shifts in p-type organic FETs during long-term bias stress[9]; however a full analysis of how the presence of water affects the performance and environmental and operational stability of high-mobility polymer FETs has not been reported yet.

The use of small, molecular additives mixed into conjugated polymer films has been explored in several previous studies. Molecular additives have been used to improve the microstructural order of solution processed polymer films[10,11] or more specifically as nucleation agents[12] to accelerate crystallization kinetics. Some groups have investigated p-type or n-type electrical doping of conjugated polymers through the addition of charge-transfer dopant molecules. For p-type doping a molecule is required with a lowest unoccupied molecular orbital (LUMO) level

deeper than the highest occupied molecular orbital (HOMO) level of the host polymer[13]. Weak-channel doping leads to better contact injection and allows tuning of the transistor threshold voltage[14] and may even improve device stability by pre-emptying electrons from filled trap states in the tail of the density of states[15]. However, it commonly leads to an undesirable increase in FET OFF current, particularly with polymer FETs where dopants cannot be confined to particular sections of the device, because they diffuse at room temperature. Here we investigate the influence of molecular additives on the environmental and operational stability as well as uniformity of high-mobility polymer FETs. Surprisingly, we have found that a wide range of molecular additives that do not act as charge transfer dopants for the polymer can dramatically improve the device stability, contact resistance and device uniformity without leading to undesirable increase in OFF current. We present a detailed study of the mechanism by which this stability improvement occurs.

We fabricated top-gate polymer FETs with a range of high-mobility conjugated donor-acceptor co-polymers and exposed them to various environments (See Methods). One of the systems we studied extensively is an indacenodithiophene-co-benzothiadiazole copolymer (IDTBT), a near amorphous polymer with a low degree of energetic disorder[4,16]. Neat IDTBT FETs without additive exhibit significant environmental instabilities and the device characteristics depend strongly on the operational environment. The as-prepared devices fabricated in a N_2 glove box had poor performance exhibiting shallow onsets and low ON currents (black curve in Fig. 1(a), left panel). When operating the devices after 24-h storage in air (blue curve), we observed much better performance with lower threshold voltage, steeper onset, and higher ON current. However, when the devices were returned to a N_2 atmosphere, performance started to degrade again (red curve); this degradation accelerated by annealing the devices in N_2 at low temperatures of 70°C (green curve). Such dependence of characteristics on the operating atmosphere constitutes a fundamental limitation for the applicability of these polymers. For example, in an OLED display package, the transistor backplane needs to operate reliably in a strictly inert, oxygen-free atmosphere to avoid OLED degradation. Surprisingly, we found

that adding 2 wt.% of the small molecule tetracyanoquinodimethane (TCNQ) to the polymer solution results in near perfect environmental stability (Fig. 1(a), right panel). Even after annealing at 70˚C for 12 hours in N_2, the characteristics retain their ideal behavior, indistinguishable from the characteristics measured after fabrication or in air. This invariance to environments can also be seen in the output characteristics, which are textbook-like and show no evidence for contact resistance (Fig. 1(b)); on the other hand, the output characteristics of devices without TCNQ depend strongly on operating environment and exhibit contact resistance limitations in the linear regime, particularly for devices operated in N_2 (Supplementary Fig. S1). We observed similar improvements for other additives, such as tetrafluoro-tetracyanoquinodimethane (F4TCNQ) and 4-aminobenzonitrile (ABN, Supplementary Fig. S2, S3). In the case of F4TCNQ the additive's electron affinity is large enough to induce some ground-state electron transfer leading to charge transfer doping, this manifests itself as an increased FET OFF current. However, for TCNQ and ABN, which have too low an electron affinity to dope IDTBT with an ionization potential of 5.3 eV (Fig. 1(c)), no increase in OFF current is observed compared to neat films.

A further benefit of additive incorporation is a significant reduction in contact resistance which we extracted from Transmission Line Method (TLM) measurements. The contact resistance of neat IDTBT transistors measured after fabrication in N_2 is high (27.1 kΩcm) and reduces to 7.1 kΩcm upon prolonged exposure to ambient air (blue to black in Fig. 1(d)). With all the molecular additives the contact resistance is below 5 kΩcm independent of environment. With TCNQ or ABN we do not see any evidence for increased bulk conductivity or OFF current suggesting that the improved contact resistance may reflect a reduction in the polymer's bulk trap density. The TLM measurements also reveal that devices with same channel lengths exhibit a significantly increased uniformity for films with additives over those without. Most notably, the spread in resistance values measured by the standard deviation (n=11 FETs on 3 substrates) is reduced by a factor of 20-30 upon incorporating 2 wt.% of F4TCNQ, TCNQ or ABN into the polymer film.

Of most critical importance for OFET applications is the operational stability over prolonged time periods. This was tested using constant-current stress measurements performed under N_2, mimicking the mode of operation in an active matrix addressed OLED display (see Supplementary Section 1 for details and measurements in air)[17]. We observed a pronounced improvement in the threshold voltage shift (ΔV_T) stability by up to a factor 12 through incorporating 2 wt.% of the molecular additives into the semiconducting film (Fig. 1(e)). In the case of F4TCNQ and ABN, ΔV_T was reduced to below 1V after a day of constant current stress under conditions representative for OLED applications. During a subsequent rest period almost complete recovery occurs, with half of the threshold voltage recovering within the first hour. This is comparable to the threshold voltage stability of established inorganic thin film transistor technologies, such as amorphous silicon[18,19] or amorphous metal oxides[20], and meets the requirements for OLED applications.

We first establish that molecular charge transfer doping is not responsible for this surprising, additive-induced stability improvement. This distinguishes our work from previous studies that reported doping to improve stability at the expense of an undesirable increase in OFF current[15]. Using ultraviolet photoelectron spectroscopy (UPS), we confirm that IDTBT and TCNQ undergo no charge transfer (Fig. 2(a)), as indeed expected from the energy level diagram. The onset of secondary electron emission, the edge of the HOMO band and hence, the position of the Fermi energy are not changing with increasing concentration of TCNQ from 0 to 20 wt.% (Supplementary Fig. S7). This is in line with the FET data (Fig. 1), where addition of TCNQ does not lead to an elevation of the OFF current that would be expected if charge transfer took place. In contrast, for the F4TCNQ additive, a small level of charge transfer does take place (Supplementary Fig. S8). This results in a small shift of the Fermi-level, which is consistent with the observed increase in OFF current and the fact that, in contrast to TCNQ, the LUMO level of F4TCNQ is slightly larger than the ionization potential of IDTBT. However, since similar enhancements in stability are observed for ABN, TCNQ, and F4TCNQ, which have a large range of electron affinities (Fig. 1(c)), this suggests that even in the case of F4TCNQ the additive-induced stability improvement is not in fact a consequence of shallow doping

observed in previous studies.[21] The UPS results are confirmed by photothermal deflection spectroscopy (PDS), a high-resolution absorption spectroscopy technique to detect sub-band gap states in organic molecules (see Methods)[22]. We find that weak charge transfer in IDTBT films with 5 wt.% of F4TCNQ leads to a clear signature of F4TCNQ anions at 1.1 eV[23] and an associated IDTBT polaron-induced absorption band between 1.2-1.6eV[4]. However, for pure IDTBT films, air exposed IDTBT films and, in particular, IDTBT films with 5 wt.% of TCNQ, additive-induced absorption features lack entirely (Fig. 2(b)). This is further evidence that charge transfer between the additive and the polymer cannot be responsible for the observed improvements in FET stability and performance. Alternatively, one could hypothesize that the additive may improve stability by undergoing charge transfer with some environmental species that would otherwise cause traps in the film; we excluded this using infrared (IR) absorption spectroscopy (Supplementary Section 4).

Inspired by these results, we investigated a wider range of molecular additives. In fact, the simplest method to incorporate a molecular additive is to leave residual solvent in the film. Residual solvents are even less likely to electronically interact with the polymer. Whilst in all previous preparations the films were annealed at 100°C for 1 hour to remove residual solvent, for these experiments neat IDTBT films were intentionally annealed for less than 2 minutes at 100°C to leave some residual solvent that can act as additive (central panel of Fig. 3(a)). Surprisingly, a similar improvement in performance and stability was observed. For IDTBT films with residual dichlorobenzene (DCB) solvent, the transfer characteristics are significantly steeper and reach higher ON-current (Fig. 3(a)) and the threshold voltage stability is significantly improved over films in which the residual solvent has been removed by annealing. Also the current-stress induced threshold voltage shift is significantly lower than in films without residual solvent (Fig. 3(b)). Solvent additives improve performance and stability similarly to solid additives; however, in contrast to TCNQ or F4-TCNQ they do not impart long-term stability as they evaporate from the films on the timescale of a month (Supplementary Fig. S15/S16).

We have observed the beneficial effect of residual solvents not only in IDTBT, but also for a wide range of high-mobility polymers. For instance, in diketopyrrolo-pyrrole (DPP) polymers, such as diketopyrrolo-pyrrole-dithienylthieno[3,2-b]thiophene (DPP-DTT)[24,25] or in polyfluorene polymers, such as poly(9,9-dioctylfluorene-alt-benzothiadiazole) (F8BT), we have observed similar improvements in performance (Fig. 3(a)) and stability (Fig. 3(b)) upon leaving residual solvents as additives in the film. In fact, with our novel preparation method, we were able to extract a gate voltage independent hole mobility of $1x10^{-2}$ cm^2/Vs for F8BT which is among the highest values reported for this material.

To better understand the molecular requirements for an additive to enhance device stability, we investigated different solvent molecules. This is possible because IDTBT, in particular, is highly soluble in a wide range of solvents. We find that many chlorinated and non-chlorinated aromatic solvents, but also non-aromatic solvents, such as chlorocyclohexane, are capable of providing this effect (Supplementary Fig. S13); a summary list is provided in Fig. 3(c). However, interestingly, some solvents, such as tetralin and 2-methylnaphthalene, only produce a limited effect or no improvement. We attribute this lack of effect to the larger size of these molecules and/or less favorable interactions of these solvents with the polymer, which manifests itself as an observed lower solubility of the polymer in these two solvents (Supplementary Section 5).

We have attempted to quantify the amount of residual solvent that remains in the film using two independent techniques, variable angle spectroscopic ellipsometry (VASE) and quartz crystal microbalance measurements. VASE measurements were performed on IDTBT films with the DCB solvent deliberately left in the film and after annealing the same films at 100°C for an additional hour (Supplementary Section 6). By fitting the data with an effective medium approximation (EMA) model that assumes a certain fraction of voids in the polymer network that are filled with a medium of refractive index n, we could significantly optimize the fits to the experimental data (Supplementary Tab. S4, Fig. S19). Optimized fits for a range of values for n, resulted in void fractions of around 1%. Interestingly, QCM

measurements on identical IDTBT films gave a consistent value of 0.9% for the amount of residual solvent (Supplementary Section 7). Assuming a void fraction of 1%, we therefore fitted the refractive index n of the void before and after removal of the residual solvent. Here, films with residual solvent could be fitted best with the void's refractive index of n=1.55 (Fig. 4(a), middle panel). This is consistent with the voids being filled by DCB which has a refractive index of 1.55. In contrast, after annealing the fitting of the experimental data resulted in a lower refractive index of n=1.2 for the voids (Fig. 4(a), bottom panel). The VASE and QCM results therefore suggest that there is a void fraction on the order of 1% in the polymer films that is largely filled with solvent after film deposition. After prolonged annealing the solvent molecules are removed from the voids which then become filled with a medium of lower refractive index, possibly a mixture of air/N_2 and water. Interestingly, the minimum concentration of TCNQ, F4TCNQ and ABN that needs to be added to the films was also on the order of 1-2 wt.%; for lower concentrations, the observed improvement in performance dropped off rapidly. We were also able to correlate the void fraction to the degree of device instability when comparing the device performance of IDTBT polymers with different side chains that exhibit different void fractions (Supplementary Fig. S21). This suggests a direct correlation between the filling of voids and device stability: As long as the voids are filled with a small molecular additive, FET performance and stability are high.

The question then arises as to the nature of the species and the physical mechanism that causes device degradation, once the voids are not filled by a molecular additive. Under such conditions significant hole trapping clearly occurs in the device: Both shallow traps that manifest themselves in reducing the sub-threshold slope and steepness of the transfer characteristics as well as deep traps that cause the current-stress induced threshold voltage shift, somehow become active. To understand the underlying mechanism, we investigated the role of water in the films[9]. Water is omnipresent in organic semiconductor films, even when devices are fabricated under inert atmospheric conditions. By exposing an IDTBT FET to humid nitrogen and dry air in an isolated cryostat, we confirmed that intentional water exposure can indeed cause similarly poor device characteristics as observed in neat IDTBT films

while exposure to O_2 is able to alleviate the adverse effect of water (Supplementary Fig. S22). To study the performance of neat IDTBT films without additive in strict absence of water, we stored the devices inside an inert glovebox with only ppm levels of H_2O, but placed the device near a powder of the strong desiccant cobalt(II) chloride (Fig. 4(b), Supplementary Section 8). Importantly, FETs exposed to $CoCl_2$ performed significantly better than reference FETs prepared in identical conditions but kept in the same glovebox away from $CoCl_2$ (Fig. 4(c)). The performance of the $CoCl_2$ exposed devices is as good as that of devices comprising an additive; also their stress stability is significantly improved over devices that were not exposed to $CoCl_2$ (Supplementary Figs. S23, S24). These experiments show that even in the absence of additives, good device performance can be obtained if water is carefully removed from the films. Under normal processing conditions, however, even if all device processing steps are carefully performed in an inert atmosphere glovebox, trace amounts of water become incorporated into the small, nanometer-sized voids within the film, when these are not filled with an additive. These water molecules are nearly impossible to remove completely by low-temperature annealing and are responsible for the poor device performance and stability of devices without molecular additive.

The formation of water-induced deep traps involved in long-term operational stress and threshold voltage shifts has been investigated previously[9]; the formation of shallow traps has mainly been studied for small molecules[26,27] , but not yet for high-mobility polymer systems. To understand the molecular mechanism by which water may create shallow hole traps in polymers, we performed electronic-structure calculations (at the optimally tuned ωB97X-D/6-31G(d,p) level of theory[28,29]) of the interactions between water molecules and the polymer backbone (See Methods and Supplementary Section 9). We present here results on IDTBT; results on DPPDTT and F8BT are shown in the Supplementary Information. The calculations involve an oligomer containing two donor-acceptor polymer repeat units; we consider its interaction with a single water molecule in two hydrogen-bonding configurations, one in which the water molecule acts as an electron acceptor / H-donor (Fig. 5(a) top panel) and the other as electron donor / H-acceptor (Fig. 5(a) bottom panel). The

results show that the presence of water strongly affects the torsional potential energy profile of the bond connecting the IDT and BT subunits. In the absence of water (black curve in Fig. 5(b)), the torsion potential is steeper than in the presence of the water molecule, particularly for the case of water acting as H-donor (red curve). The decreased potential energy barrier induced by water causes a marked decrease in the system order, a much wider distribution of torsion angles and a broader distribution of HOMO energies over *ca*. 200 meV (Supplementary Tab. S6). As a result, shallow trap states appear for the positively charged hole carriers. This is consistent with our previously reported finding that in poorly crystalline but high-mobility polymers a narrow, well-defined distribution of torsion angles is the origin of high performance[4]. We expect the electrical performance of this type of polymers to be highly sensitive to any mechanism that widens the distribution of torsion angles and thus creates a distribution of shallow trap states, which is in line with the poor performance of devices without additive.

There are other potential mechanisms by which water molecules can cause charge trapping: We have considered the solvation of positive polarons by polar water molecules (Fig. 5(c)) and have found that the polarization interaction energy of the polaron per water molecule is comparable, though of slightly smaller magnitude, than the interaction energy between the neutral chain and a water molecule that we discussed above (supplementary Section 9). Therefore, solvation effects are unlikely to dominate, but could contribute to shallow trap formation. For deep trap formation the production of protons H^+ by the electrochemical reaction of holes (h^+) on the polymer with water molecules $2H_2O + 4h^+ \rightarrow 4H^+ + O_2$ has been suggested as the main mechanism for bias-stress induced degradation in OFETs[9]. In our calculation there is no indication that water (or an H_2O-O_2 complex) can transfer an electron to a hole (positive polaron) on the polymer chains (the ionization potential of water or water-O_2 being much larger than the electron affinity of a positive polaron on the backbone). However, the situation changes in the case of hydroxyl anion formation (leaving behind a proton or hydronium cation). The calculations show that a hydroxyl anion has a sufficiently low ionization potential that it can readily transfer an electron to a positive polaron, as illustrated in Fig. 5(d), leading to

the loss of the polaron. The resulting OH radical can be expected to be amenable to further reactions to eventually generate oxygen and additional protons. Thus, this electrochemical mechanism is likely to play a role as well provided that some hydroxyl anions from the water dissociation reaction are present within the polymer's voids. Though our calculations do not allow us to identify a single dominant mechanism they make it very clear that water can be expected to degrade device performance and stability through several potential mechanisms.

In terms of the mechanism for the additive-induced improvements in stability we propose two hypotheses: (i) the additives interact with the polymer in a way that they restore the steepness of the torsion potential; and/or (ii) they simply displace water molecules from direct contact with the polymer and thus, prevent any of the discussed trap formation pathways or render them less effective. To investigate these mechanisms we also performed electronic-structure calculations in which both a water molecule and an additive molecule interact with the polymer; however, the conformational space that needs to be considered at the electronic-structure level becomes so vast that it would be difficult to identify the relevant, low-energy configurations (Supplementary Section 9). The fact that oxygen has a beneficial, "water-passivating" effect as well, can be related to the formation of hydrogen-bonded water-oxygen complexes (such as (H_2O-O_2) or ($[H_2O]_2$-O_2))[8] that could similarly prevent water from interacting directly with the polymer chains.

Experimentally, the molecular configurations within the small voids are very difficult to probe, as the relevant concentrations of water involved are low while simultaneously water is omnipresent in most experiments. In any case, our work has clearly demonstrated the significant benefit that molecular additives exert on the performance and stability of state-of-the-art polymer FETs. It provides a practical and manufacturable technique to resolve a long-standing challenge in polymer electronics; the operational and environmental stability achieved through the addition of molecular additives will enable a wider range of applications for polymer electronics, including advanced OLED and liquid crystal displays, as well as FET sensors that should be sensitive only to the analyte but not to changes in the

operational conditions. Our simple additive-induced trap removal technique is also likely to benefit other applications of organic semiconductors such as charge transport in light-emitting diodes or solar cells.

Methods:

Device fabrication

Top-gate bottom contact field effect transistors were fabricated on glass substrates with photo-lithographically defined electrodes of Ti/Au (10 nm/ 30 nm). Polymers were then deposited by spin coating, followed by an annealing step at 100 ºC for 60 minutes to drive out residual solvent from the film. To leave residual solvent in the film intentionally, annealing was done for 2 minutes only. For devices comprising a solid additive (TCNQ, F4TCNQ or ABN), the material was added to the polymer solution in the range from 1-20wt. %. For a dielectric layer, a 500 nm layer of Cytop (Asahi Glass) was spin coated (Cytop was annealed at 80 °C for 15 minutes) and devices were finished off by evaporating a 20nm thick aluminium top gate through a shadow mask. Transistor transfer characteristics were measured with an Agilent 4155B Semiconductor Parameter Analyser. To guarantee reproducibility, all fabrication steps as well as all electrical measurements were performed in a N_2 glove box.

The environmental stability of OFETs was investigated on devices fabricated in a nitrogen environment. For all devices the same measurement protocol was applied:

(i) OFETs were characterized in a N_2 glove box directly after fabrication by recording linear and saturation transfer characteristics as well as output characteristics.

(ii) Devices were exposed in the dark (to exclude effects of light) to air for 24 hours, transferred to nitrogen and characterized immediately afterwards. Here, the samples were characterized on the same setup as in (i).

(iii) Devices were stored in a N_2 glove box for 24 hours and characterized subsequently

(iv) Samples were heated for 12 hours in nitrogen at 80C (to accelerate degradation) and were characterized thereafter.

More details on operational current-stress measurements are furthermore given in Supplementary Section 1.

Ultraviolet photoelectron spectroscopy (UPS)

UPS was used to determine the position of the Fermi level E_F of IDTBT with various additives. The system operates by emitting photons of a fixed energy of 21.2eV (58.4 nm) via a helium gas-discharge lamp. Based on Einstein's photoelectric law, photoelectrons are able to escape from the surface of a sample if their kinetic energy is sufficient to overcome the sum of the binding energy of their initial level (taken with reference to E_F) and the material's workfunction $\Phi = E_{VAC} - E_F$. Here, the secondary electron cut-off represents electrons without any kinetic energy. Consequently, a material's Fermi level position with respect to the vacuum level (its workfunction) can be computed by determining the secondary electron cut off from a UPS spectrum and subtracting it from the incident photon energy adjusted for any external potential applied during the measurement (-5V for all results presented herein).

Photothermal deflection spectroscopy (PDS)

A PDS set-up was used to measure sub-band gap absorptions. This technique is based on the heat energy that is released from the surface of the sample when monochromatic light is absorbed. An inert liquid surrounding the sample dissipates this thermal energy, changes its refractive index and consequently deflects a laser beam which is sent at grazing incidence along the surface of the substrate. Using a quadrant detector connected to a lock-in amplifier, the deflection of the laser beam

is recorded as a function of the monochromatic pump wavelength, resulting in a reading of absorbance.

Variable angle spectroscopic ellipsometry (VASE) measurements

The VASE measurements were performed in reflection geometry using a variable angle M-2000 spectroscopic ellipsometer with rotating compensator (J. Woollam Co.) in the wavelength range from 400nm to 900nm and angles of incidence from 50 - 70 degrees relative to the substrate normal on samples prepared on Si (100) with a native oxide layer of 2nm thickness. More details on the analysis of the ellipsometric raw data are given in Supplementary Section 6.

Computational Information

All calculations were carried out at the Density Functional Theory (DFT) level with the Gaussian09 code.[30] We used the long-range corrected ωB97X-D functional, with the long-range separation parameter ω optimized for each system based on the ionization-potential tuning method.[28,29] Effects related to the surrounding medium were approximated by the integral equation formalism - polarizable continuum model (IEFPCM) model, which accounts for polarity of the surrounding medium in an isotropic way. The dielectric constant was chosen as 3.5, which is a representative value for organic materials.[31] The procedure followed was: (i) to optimize the oligomer geometry using the ωB97X-D/6-31G(d,p) method; (ii) to tune the ω-value for the isolated system ("in the gas phase"); and (iii) to re-optimize the geometry with the gas-phase tuned-ωB97X-D functional while now including IEFPCM. The ω-value found in the aforementioned procedure was used in all further calculations since the perturbations to this value by adding to the system a small molecule, in this case water, are minimal.

Acknowledgements:

We gratefully acknowledge financial support from Innovate UK (PORSCHED project) and the Engineering and Physical Sciences Research Council though a Programme Grant (EP/M005141/1). I.N. acknowledges studentship support from FlexEnable Ltd. K.B. gratefully acknowledges financial support from the Deutsche Forschungsgemeinschaft (BR 4869/1-1). B.R., M.K.R., and J.L.B. thank the financial support from King Abdullah University of Science and Technology (KAUST), the KAUST Competitive Research Grant program, and the Office of Naval Research Global (Award N62909-15-1-2003); they also acknowledge the IT Research Computing Team and Supercomputing Laboratory at KAUST for providing computational and storage resources.

References:

1. Sokolov, A. N. *et al.* From computational discovery to experimental characterization of a high hole mobility organic crystal. *Nat. Commun.* **2,** 437 (2011).

2. Nielsen, C. B., Turbiez, M. & McCulloch, I. Recent advances in the development of semiconducting DPP-containing polymers for transistor applications. *Adv. Mater.* **25,** 1859–1880 (2013).

3. Himmelberger, S. & Salleo, A. Engineering semiconducting polymers for efficient charge transport. *MRS Commun.* **5,** 1–13 (2015).

4. Venkateshvaran, D. *et al.* Approaching disorder-free transport in high-mobility conjugated polymers. *Nature* **515,** 384–388 (2014).

5. Kim, G. *et al.* A thienoisoindigo-naphthalene polymer with ultrahigh mobility of 14.4 cm2/V·s that substantially exceeds benchmark values for amorphous silicon semiconductors. *J. Am. Chem. Soc.* **136,** 9477–9483 (2014).

6. Soon, Y. W. *et al.* Material crystallinity as a determinant of triplet dynamics and oxygen quenching in donor polymers for organic photovoltaic devices. *Adv. Funct. Mater.* **24,** 1474–1482 (2014).

7. Chua, L. *et al.* General observation of n-type field-effect behaviour in organic semiconductors. *Nature* **434,** 194–9 (2005).

8. Nicolai, H. T. *et al.* Unification of trap-limited electron transport in semiconducting polymers. *Nat. Mater.* **11,** 882–887 (2012).

9. Bobbert, P. A., Sharma, A., Mathijssen, S. G. J., Kemerink, M. & De Leeuw, D. M. Operational stability of organic field-effect transistors. *Adv. Mater.* **24,** 1146–1158 (2012).

10. Lee, J. K. *et al.* Processing additives for improved efficiency from bulk heterojunction solar cells. *J. Am. Chem. Soc.* 3619–3623 (2008). doi:10.1021/ja710079w

11. Peet, J., Senatore, M. L., Heeger, A. J. & Bazan, G. C. The role of processing in the fabrication and optimization of plastic solar cells. *Adv. Mater.* **21,** 1521–1527 (2009).

12. Treat, N. D. *et al.* Microstructure formation in molecular and polymer semiconductors assisted by nucleation agents. *Nat. Mater.* **12,** 628–633 (2013).

13. Lüssem, B., Riede, M. & Leo, K. *Doping of organic semiconductors*. *Physica Status Solidi (A) Applications and Materials Science* **210,** (2013).

14. Lüssem, B. *et al.* Doped organic transistors operating in the inversion and depletion regime. *Nat. Commun.* **4,** 1–6 (2013).

15. Hein, M. P. *et al.* Molecular doping for control of gate bias stress in organic thin film transistors. *Appl. Phys. Lett.* **104,** (2014).

16. Zhang, W. *et al.* Indacenodithiophene semiconducting polymers for high performance air stable transistors. *J. Am. Chem. Soc.* 11437–11439 (2010).

17. Sirringhaus, H. 25th anniversary article: Organic field-effect transistors: The path beyond amorphous silicon. *Adv. Mater.* **26,** 1319–1335 (2014).

18. Sirringhaus, H. Reliability of Organic Field-Effect Transistors. *Adv. Mater.* **21,** 3859–3873 (2009).

19. Hekmatshoar, B., Wagner, S. & Sturm, J. C. Tradeoff regimes of lifetime in amorphous silicon thin-film transistors and a universal lifetime comparison framework. *Appl. Phys. Lett.* **95,** 3–5 (2009).

20. Kim, S. Il *et al.* High Reliable and Manufacturable Gallium Indium Zinc Oxide Thin-Film Transistors Using the Double Layers as an Active Layer. *J. Electrochem. Soc.* **156,** H184 (2009).

21. Olthof, S. *et al.* Ultralow doping in organic semiconductors: Evidence of trap filling. *Phys. Rev. Lett.* **109,** 1–5 (2012).

22. Buchaca-Domingo, E. *et al.* Direct correlation of charge transfer absorption with molecular donor:acceptor interfacial area via photothermal deflection spectroscopy. *J. Am. Chem. Soc.* **7,** 150409144253004 (2015).

23. Pingel, P. & Neher, D. Comprehensive picture of p-type doping of P3HT with the molecular acceptor F4TCNQ. *Phys. Rev. B - Condens. Matter Mater. Phys.* **87,** 1–9 (2013).

24. Li, J. *et al.* A stable solution-processed polymer semiconductor with record high-mobility for printed transistors. *Sci. Rep.* **2,** 1–9 (2012).

25. Xu, H. *et al.* Spectroscopic Study of Electron and Hole Polarons in a High-Mobility Donor - Acceptor Conjugated Copolymer. *J. Phys. Chem. C* 130305161117003 (2013). doi:10.1021/jp4003388

26. Cramer, T. *et al.* Water-induced polaron formation at the pentacene surface: Quantum mechanical molecular mechanics simulations. *Phys. Rev. B - Condens. Matter Mater. Phys.* **79,** 1–10 (2009).

27. Tsetseris, L. & Pantelides, S. T. Intercalation of oxygen and water molecules in pentacene crystals: First-principles calculations. *Phys. Rev. B - Condens. Matter Mater. Phys.* **75,** 1–4 (2007).

28. Chai, J.-D. & Head-Gordon, M. Long-range corrected hybrid density functionals with damped atom-atom dispersion corrections. *Phys. Chem. Chem. Phys.* **10,** 6615–6620 (2008).

29. Körzdörfer, T. & Bredas, J. L. Organic electronic materials: Recent advances in the dft description of the ground and excited states using tuned range-separated hybrid functionals. *Acc. Chem. Res.* **47,** 3284–3291 (2014).

30. Frisch, M. J. *et al. Gaussian 09*. (Gaussian, Inc., 2009).

31. Schwenn, P. E., Burn, P. L. & Powell, B. J. Calculation of solid state molecular ionisation energies and electron affinities for organic semiconductors. *Org. Electron.* **12,** 394–403 (2011).

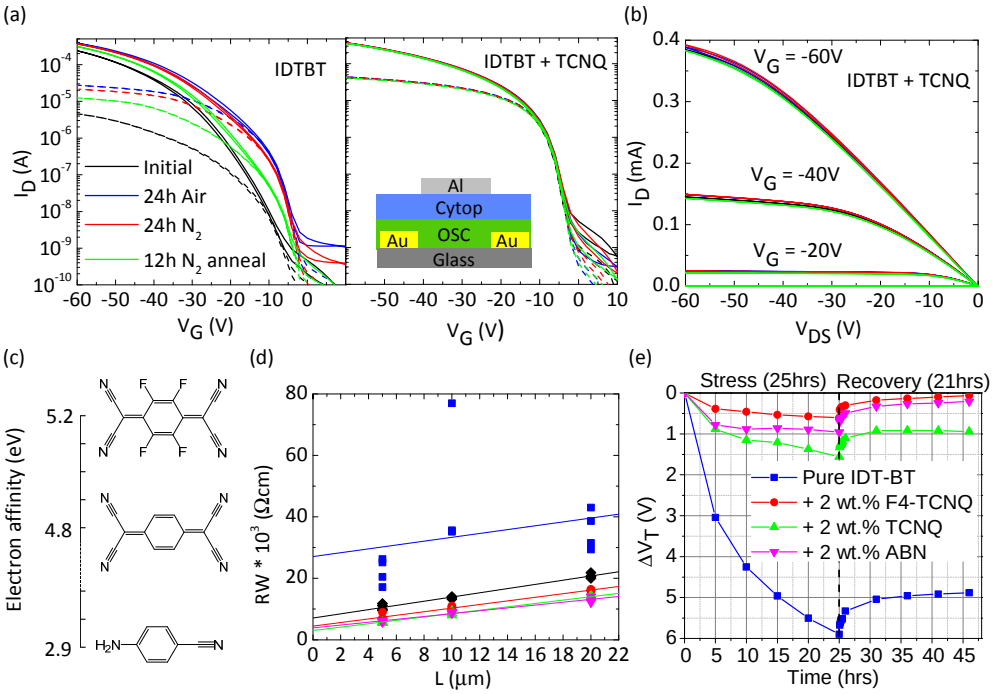

Figure 1 Improving polymer FET performance and the environmental and operational stability through the use of molecular additives (a) Linear (V_{DS} = -5V, dashed lines) and saturation (V_{DS} = -50V, solid lines) transfer characteristics of IDTBT OFETs with (right panel) and without (left panel) 2 wt.% of TCNQ additive. Measurements were taken successively for the as-prepared device, after 24 hours exposure to first air and then nitrogen environments and after a 12 h anneal in nitrogen. The device structure is shown as an inset (channel length *L* = 20 μm, channel width *W* = 1 mm); (b) Output characteristics of an OFET with 2 wt.% of TCNQ additive; (c) Electron affinity of the F4TCNQ (top), TCNQ (middle) and ABN (bottom) additives used; (d) Transmission line measurements of the normalized channel resistance as a function of channel length for FETs comprising IDTBT (blue squares), IDTBT after air exposure (black diamonds) and IDTBT with 2 wt.% of TCNQ (green triangles), ABN (magenta triangles) or F4TCNQ (red circles). The contact resistance can be extracted from an extrapolation to zero channel length; (e) Constant current-stress measurements at 2.5μA and room temperature comparing the threshold voltage shift of neat IDTBT OFETs with and without additives, in nitrogen. The recovery kinetics after removing the current stress are also shown.

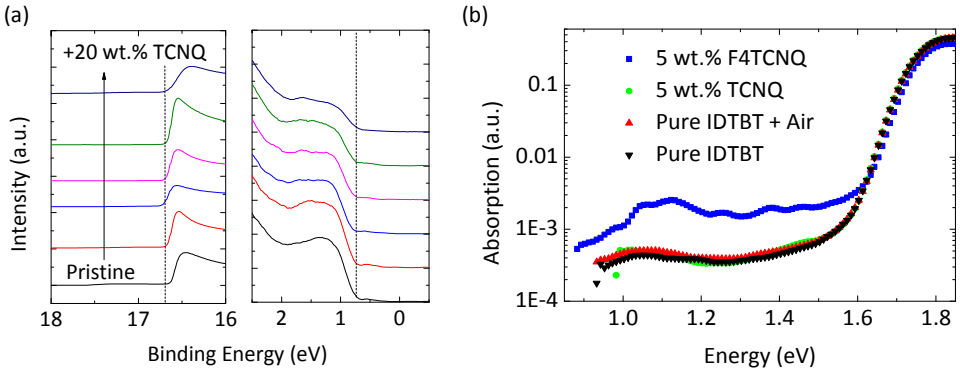

553

554 **Figure 2 Investigation of potential electronic interactions between additives and**
555 **the polymer** (a) UPS measurements near the cut-off for secondary electron emission
556 (left) and near the HOMO edge (right) for IDTBT films with 0,1,2,5,10,20 wt.% of
557 TCNQ; (b) PDS spectra of IDTBT with and without 5 wt.% of F4TCNQ and TCNQ. The
558 spectrum of a neat IDTBT film after exposure to air is also shown.

559
560
561
562
563
564
565

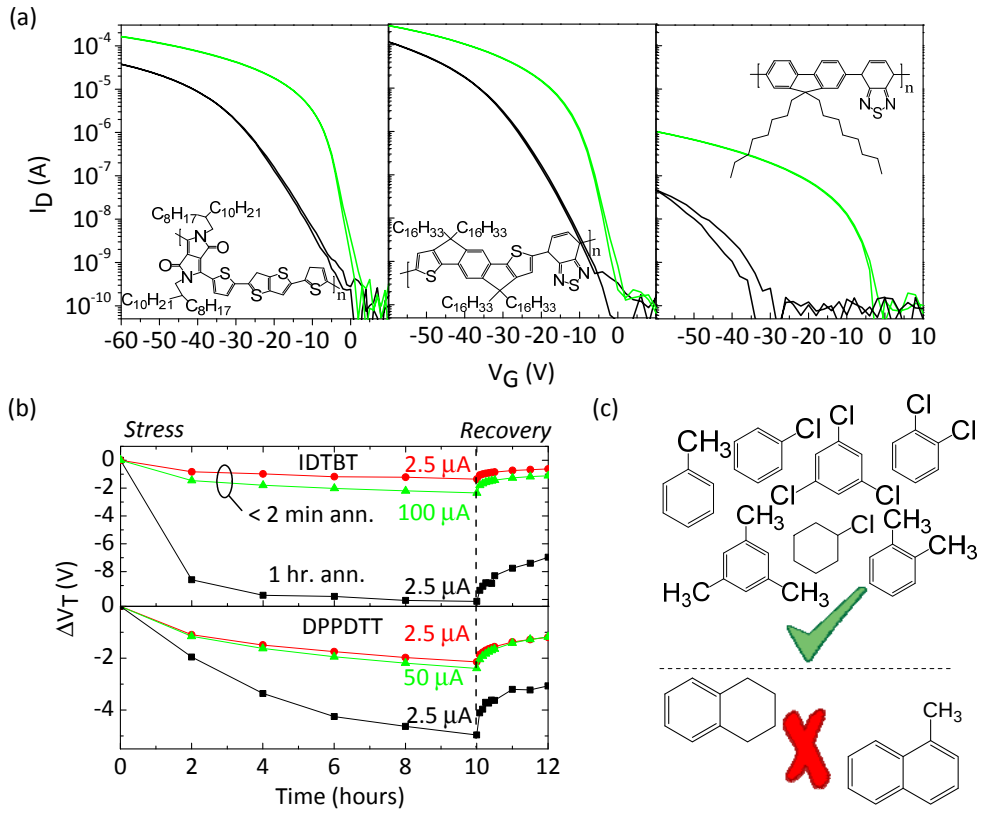

Figure 3 Effect of residual solvents on polymer FET performance and stability (a) Improvement of the saturation transfer characteristics (V_{DS} = -50V) for DPP-D-TT (left, structure shown), IDTBT (center, structure shown) and F8BT (right, structure shown) FETs by leaving residual solvent (DCB) in the polymer film as an additive. Films were annealed for < 2min at 100°C leaving residual solvent in the film (green lines) or for 1 hour to remove residual solvent (black lines); (b) Comparison of current-stress stability of IDTBT (top) and DPPDTT FETs with and without residual solvent in the polymer films; to confirm that increased stress-stabilities are unrelated to the lower voltages that need to be applied to devices with residual solvent to maintain a constant current of 2.5 µA, we also stressed the device at a much higher current (100 µA for IDTBT and 50 µA for DPPDTT), and even under these aggressive conditions the threshold voltage shift is smaller than that of a device without residual solvent stressed at 2.5 µA; (c) List of solvents that lead to performance and stability improvement if left in films of IDTBT (top) as well as solvents that do not show a beneficial effect on device stability and performance (bottom).

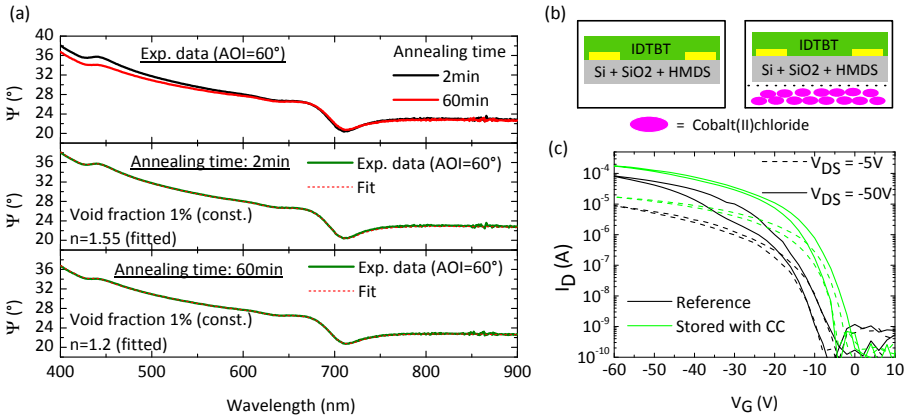

Figure 4 Interaction of water with polymer semiconductors (a) Experimental VASE data for an IDTBT film after 2 and 60 minutes of annealing (top). Experimental data after 2min (middle) and 60min (bottom) of annealing fitted with an effective medium approximation (EMA) model fitting the refractive index of voids in the polymer assuming a void fraction of 1% consistent with QCM measurements. (b) Schematic diagram of the experiment used for strictly removing water from an IDTBT transistor with cobalt(II) chloride powder (c) IDTBT bottom-gate OFET treated with Cobalt(II) Chloride powder as compared to a reference device.

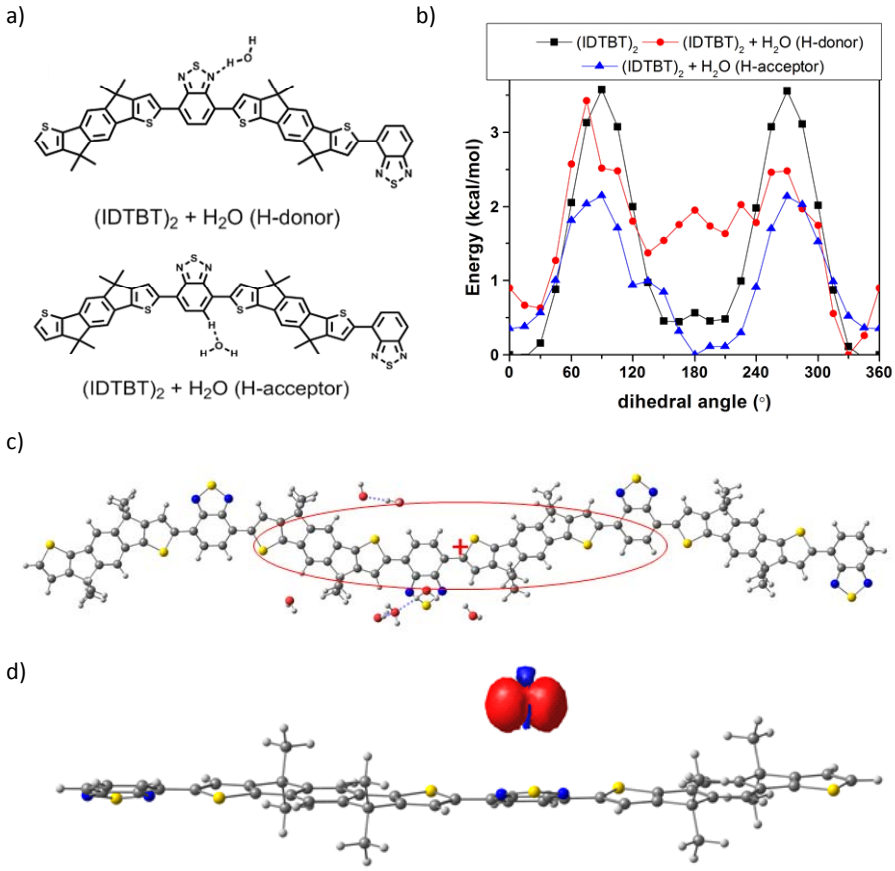

Figure 5 Computational evaluation of the interaction between a water molecule and the polymer backbone (a) Chemical structures of $(IDTBT)_2$–H_2O complexes with water acting as H-donor or H-acceptor; (b) torsional potential of the bond bridging the central IDT and BT units in the absence and presence of water; (c) illustration of the interaction between a positive polaron (polaron wavefunction represented schematically with a red oval) and water molecules (the calculated average interaction energy per water molecule is given in the SI); (d) illustration of the electron transfer between an hydroxyl anion and a positive polaron, which leads to an hydroxyl radical (whose spin density is represented) and the loss of the polaron (see SI for full details). All calculations incorporate the effect of the surrounding medium (IEF-PCM model with ε=3.5) and were performed at the tuned ωB97X-D level of theory.